International Journal of Applied Pharmaceutics

ISSN- 0975-7058 Vol 17, Issue 4, 2025

Original Article

DEVELOPMENT AND OPTIMIZATION OF ARNEBIN-1 LOADED THERMOSENSITIVE HYDROGEL FOR WOUND HEALING

RAHUL GODGE[1*], KAILAS BARDE[1], ONKAR PAWAR[1], SANTOSH DIGHE[2]

[1]Department of Pharmaceutical Quality Assurance, Pravara Rural College of Pharmacy, Loni, India. [2]Department of Pharmacology, Pravara Rural College of Pharmacy, Loni, India

*Corresponding author: Rahul Godge; *Email: rahulgodge@gmail.com

Received: 02 Mar 2025, Revised and Accepted: 14 Apr 2025

ABSTRACT

Objective: To develop and optimize an arnebin-1-loaded thermosensitive hydrogel for enhanced wound healing applications. Current wound dressing methods lack purposes such as proper moisture regulation and suitable antimicrobial properties combined with inadequate drug delivery systems and poor patient usage. The novel arnebin-1 containing thermosensitive hydrogel employs sustained drug delivery and antimicrobial functions to solve current wound dressing issues.

Methods: A 3^2 full factorial design was employed to develop thermosensitive hydrogels using Poloxamer 407 and Pectin as key variables. Nine formulations were systematically evaluated through response surface methodology, optimizing critical parameters of gelling temperature and mucoadhesive strength. Comprehensive characterization included physicochemical properties, ex-vivo permeation, stability studies, and antimicrobial assessment against common wound pathogens *(E. coli and S. aureus).*

Results: Among nine formulations, KF6 emerged as the optimal formulation through desirability function approach (desirability = 1.0), containing Poloxamer 407 (36% w/v) and Pectin (0.9% w/v). KF6 demonstrated ideal physiological gelation (34.6±0.3 °C), enhanced mucoadhesion (4156±204 dynes/cm^2), and sustained drug release (95.4% over 12 h). The formulation exhibited superior drug permeation (flux: 152.68±4.58 µg/cm^2/hr), significant antibacterial activity against *S. aureus* (16.8±0.9 mm) and E. coli (14.2±0.7 mm) and maintained stability for three months under various storage conditions.

Conclusion: The optimized thermosensitive hydrogel presents a promising platform for clinical wound management, offering advantages of ease of application, sustained drug delivery, and significant antimicrobial activity. This novel formulation provides a potential alternative to conventional wound dressings, warranting further clinical investigation for translation into therapeutic applications.

Keywords: Arnebin-1, Thermosensitive hydrogel, Wound healing, Response surface methodology, Ex-vivo permeation, Antibacterial activity, Clinical translation

DOI: https://dx.doi.org/10.22159/ijap.2025v17i4.54107 Journal homepage: https://innovareacademics.in/journals/index.php/ijap

INTRODUCTION

Chronic and acute wounds are a major global health concern and their contributing factor is estimated to cost millions of dollars to the world healthcare organizations [1]. Surgical cuts and various other injuries such as diabetic ulcers can be classified into acute and chronic and must therefore be approached in a correct procedure to avoid a deterioration of their condition [2]. Wound healing can be defined as the complex series of events that occur during three main phases that include inflammation, proliferation, and tissue remodelling [3]. However, the wound healing may be hindered by certain factors such as infection, oxidative stress, organism's poor circulation etc [4]. In the current durations epidemiological investigations, chronic wounds have been estimated to occur in about 2% of residents in the developed nations and the incidences are higher in the elderly and diabetic patients [5]. The enhanced rates of chronic wounds along with the growing cases of antibiotic resistant bacterial strains has prompted the need for novel therapeutic options that are effective in wound healing and possess antimicrobial properties [6].

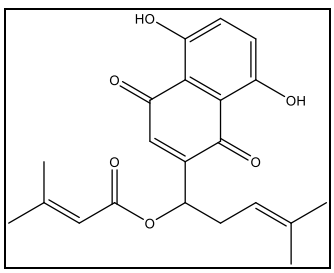

Fig. 1: Chemical structure of Arnebin-1

Arnebin-1 obtained from Arnebiaeuchroma has been identified as a potent naphthoquinone for the potential application in wound healing [7]. The therapeutic potential of arnebin-1 for wound healing applications is high because this compound exhibits robust pharmacological characteristics along with proven antimicrobial and anti-inflammatory effects [8]. Scientific experiments prove that VEGF and bFGF expression levels rise by 1.8-fold and 2.3-fold respectively when analyzing arnebin-1 treated cells compared to untreated ones thereby enhancing tissue regeneration through increased angiogenesis. The application of arnebin-1 to wounds at 10-50 µg/ml triggers fibroblast population growth while raising collagen levels by 40% better than untreated skin while lower cytokines TNF-α and IL-6 reach 35-45% decrease [9]. These multi-faceted mechanisms position arnebin-1 as superior to conventional single-action antimicrobial agents used in wound care [10].

Thermosensitive hydrogels as a new generation of drug delivery systems, which can gel in physiological temperature, has special application prospect on wound healing [11]. These smart materials are more advantageous than both solutions and gels: they are easy to apply since they can be provided as a liquid at room temperature and transform into a gel on contact with the wound. Hydrogels with a three-dimensional network formation offer an appropriate environment for wound healing while providing permeability for getting oxygen and nutrients [12]. In addition, thermosensitive hydrogels can be faced with the ability to provide controlled drug release meaning the drug concentration remains optimal at the wound site for quite some time [13]. Wound healing research has advanced however standard wound coverings continue to encounter numerous problems particularly within chronic wound management. Wounds do not receive sufficient steady drug levels at the site because existing treatment methods succeed inconsistently which leads to ineffectiveness and greater susceptibility to infections. The majority of

traditional wound dressings deliver only one of their key functions as moisture control or antimicrobial protection but do not provide advanced dual capabilities. The current approaches to treatment demand regular dressing adjustments that lead to healing delays and cause physical discomfort to patients. The medical benefits of thermosensitive hydrogels surpass traditional dressings through their ease of temperature-controlled administration then their ability to form at body temperature and their controlled medication delivery and their ability to manage liquid content in wounds. The thermosensitive hydrogel system provides sustained drug delivery at the wound site which enables fewer treatment applications hence enhancing patient compliance [14].

The objective of this work is to design and characterise an arnebin-1 incorporating thermosensitive hydrogel system for advanced wound healing therapy. Particularly the physicochemical properties, in vitro drug release and bactericidal effects against bacteria related to wound infection. This study offers an innovative solution to the drawbacks related to conventional arnebin-1 delivery and at the same time takes advantage of the use of thermosensitive hydrogels for wound healing purposes.

MATERIALS AND METHODS

Materials

Arnebin-1 (purity ≥98% by HPLC) was procured from Sciquaint Innovations Private Limited (Pune, India). Poloxamer 407 (Kolliphor® P 407, average molecular weight 12,600, PEO98-PPO67-PEO98) was obtained from Neeta Chemicals (Pune, India). Pectin (degree of esterification 65-70%, galacturonic acid content ≥74%) was purchased from Research Lab Fine Chem Industries (Mumbai, India). Analytical grade phosphate buffer (pH 6.8), ethanol (≥99.5% purity), and dimethyl sulfoxide (DMSO, ≥99.9% purity) were procured from Merck Limited (Mumbai, India). All other chemicals and reagents used were of analytical grade and used as received without further purification. Double distilled water was used throughout the study.

Methods

Calibration curve of arnebin-1

Arnebin-1 was dissolved in Phosphate Buffer pH 6.8 to determine their spectral properties as shown below. For this purpose, 10 mg of pure drug sample of Arnebin-1 was taken in 100 ml (100 µg/ml) of the calibrated volumetric flask, dissolved and made up to the mark with Phosphate Buffer of pH 6.8. It was the stock solution of Arnebin-1 (100 µg/ml) dissolved in phosphate buffer solution of pH 6.8 [15]. The working standard solution of 100 µg/ml was prepared from the stock solution as follows; To prepare different working standard solutions of the range (5-30 µg/ml), aliquots (0.5, 1.0, 1.5, 2.0, 2.5, and 3.0 ml) of the stock solution were pipette into 10 ml of calibrated volumetric flask, all of which were made up to the mark with phosphate buffer of pH 6.8. The absorbance of each solution was read at the wavelength of 288.3 nm in UV-1900 Shimadzu spectrophotometer as it was observed to have the highest absorbance in the UV spectrum [16].

QbD approach for formulation design

A 3^2 full factorial design was selected for optimizing the thermosensitive hydrogel formulation. This design efficiently evaluates two critical factors at three levels with minimal experimental runs while capturing non-linear relationships, providing comprehensive coverage of the experimental space with sufficient degrees of freedom for evaluating main effects and factor interactions. The independent variables studied were concentrations of Poloxamer 407 (A) and Pectin (B), each at three levels: low (-1), medium (0), and high (+1). The dependent variables investigated were gelling temperature (°C) (Y^1) and Mucoadhesive strength (dynes/cm^2) (Y^2). Nine formulations were generated using Design Expert software (version 13.0, Stat-Ease Inc., Minneapolis, MN, USA), with experimental runs and formulation designs presented in tables 1 and 2 [17, 18]. Preliminary studies and literature review guided the selection of Poloxamer 407 concentrations from 30-36% w/v and Pectin concentrations from 0.6-1.2% w/v. Poloxamer 407 served as the main thermosensitive agent because it undergoes sol-gel phase transitions that reverse at different temperatures however 30% w/v was not sufficient for gel formation and 36% w/v created excessive viscosity at both room temperature conditions. The mucoadhesive agent and structure stabilizer Pectin was incorporated at specific concentrations that optimized both the time the formulation stayed at the wound site and the formulation's fluidity at room temperature.

The following quadratic model equations were used to evaluate the responses:

$$Y = \beta_0 + \beta_1 A + \beta_2 B + \beta_{12} AB + \beta_{11} A^2 + \beta_{22} B^2 + \varepsilon \ldots\ldots (1)$$

Where, Y represents the response (Y1 or Y2), β_0 is the arithmetic mean response, β_1 and β_2 are the coefficients for factors A and B respectively, β_{12} represents the interaction coefficient, β_{11} and β_{22} are the coefficients for quadratic terms, ε is the residual error.

Table 1: 3^2 Factorial design showing independent factors and levels

Independent variables				
Label	**Factors**	**Level (mg)**		
		Low (-)	**Medium**	**High (+)**
A	Poloxamer 407 (% w/v)	30	33	36
B	Pectin (% w/v)	0.6	0.9	1.2
Dependant variables				
Y_1	Gelling temperature (C)			
Y_2	Mucoadhesive strength (dynes/cm^2)			

Table 2: Preparation of thermosensitive hydrogel batches using 3^2 factorial designs

Ingredients	KF1	KF2	KF3	KF4	KF5	KF6	KF7	KF8	KF9
Arnebin-1 (mg)	100	100	100	100	100	100	100	100	100
Poloxamer 407 (% w/v)	30	33	36	30	33	36	30	33	36
Pectin (% w/v)	0.6	0.6	0.6	0.9	0.9	0.9	1.2	1.2	1.2
Distilled Water (%)	q. s. to 100	q. s. to 100	q. s. to 100	q. s. to 100	q. s. to 100	q. s. to 100	q. s. to 100	q. s. to 100	q. s. to 100

Preparation of thermosensitive hydrogel

Thermosensitive hydrogel was synthesized through cold method. Arnebin-1 (100 mg) was first dissolved in a minimal volume of DMSO (2 ml, 50 mg/ml concentration) under gentle magnetic stirring (200 rpm for 15 min at room temperature) to ensure complete solubilisation while minimising the final DMSO content in the formulation to less than 5% v/v. Poloxamer 407 followed by (30-36% w/v) and Pectin followed by (0.6-1.2% w/v) were dissolved in cold phosphate buffer (the pH=6.8, 4 °C with magnetic stirrer at 400

rpm. The polymer solutions were allowed to hydrate at the temperature of 4 °C for a period of 24 h. The Arnebin-1 solution was then added to the cold polymer solution in a drop-wise manner with constant stirring to avoid instantaneous gelation of the polymer and the temperature was kept at 4 °C during the process. The mixing was continued for 30 min at 4 °C to ensure uniform distribution of all components. The final volume was adjusted to 100 ml with cold phosphate buffer (pH 6.8) and the formulation was left standing at 4 °C for 24 h for complete hydration and to eliminate air bubbles, resulting in a homogeneous gel system with 1 mg/ml final arnebin-1 concentration. To achieve this, nine formulations were prepared with the different concentrations of Poloxamer 407 (30%, 33%, and 36% w/v) and Pectin (0.6%, 0.9%, and 1.2% w/v) while Arnebin-1 concentration remains constant (100 mg) [12, 19].

Characterization of thermosensitive hydrogel

Fourier Transform Infrared analysis

FTIR analysis was carried out with a Shimadzu IR Affinity-1 instrument (Japan) fitted with ATR accessory. All the samples including pure arnebin-1, Poloxamer 407, pectin and the optimized hydrogel formulation were scanned in the region of 4000-400 cm^{-1} with a resolution of 4 cm^{-1} and with 32 scans [20]. In these, the peak values were identified and there were also investigations on the possible interactions between the drug and polymers.

Differential scanning calorimetry analysis

DSC analysis was performed on a DSC60-PLUS thermal analyzer (Shimadzu Co. LTD, Japan). About 5-10 mg quantities of pure arnebin-1, Poloxamer 407, pectin, and the optimum formulation of hydrogel were weighed separately in triplicate in an alu-alu foil pan incorporating a T-groove and sealed hermetically. The samples were heated from 25 °C to 300 °C with a scanning rate of 10 °C/min, under nitrogen flow of 50 ml/min. For reference, a shiny surface, an empty aluminum pan was also used. The thermograms obtained were then characterized for thermal events and drug-polymer interactions [21].

Texture analysis

The texture profile analysis was done using a Texturer model TA. XT plus (Stable Micro Systems Limited, UK) which has a control unit and static force measuring unit of 5 kg and a cylindrical probe of 25 mm diameter. The formulations (20 g) were placed in standard containers at room temperature of 25±0.5 °C. The probe was drawn down at a speed of 0.5 mm/s when the penetration depth was up to 10 mm. All the tests and measurements such as hardness, cohesiveness, and adhesiveness were taken and recorded three times to get average values, and force time curves were analyzed by using the software of Texture Expert [22].

Gelling temperature

The gelation temperature was also found out using the tube inversion technique. While for dissolution, sample vials containing 2 ml of the formulation were placed in water-bath maintained with the help of Remi Equipment Manufacture India. The temperature was set at an increase of 1 °C/min starting from 20 °C in order to reach 40 °C at the end. For each temperature point, the vials were inverted so that it formed the 90° and the gelling temperature was obtained as the temperature range in which the solution could not flow for half a minute. Measurements were performed in triplicate [23].

Gelling time

Gelling time was determined using the vial tilting technique at 37±0.5 °C. Two milliliters of the formulation was dispensed into separate vials and then exposed to physiological temperature water bath. After 30 seconds the vials were rotated at 90° intervals until the gelation was obtained. The gelling time was determined as the time it took for the solution to cease from dripping when tilted. Each measurement was repeated three times so as to obtain reproducible results [24].

Viscosity

All the viscosity assessments were done using a Brookfield viscometer (DV-II+Pro, Brookfield Engineering Laboratories, USA) with spindle CP-52. Sample temperature was regulated, and a circulating water bath was used to maintain the appropriate temperature. The analyses were conducted at both room and physiological temperatures (25±0.5 and 37±0.5 °C, respectively) across a range of shear rates (0.5, 5, 10, 30, and 100 RPM, corresponding to 0.83, 8.3, 16.7, 50.0, and 166.7 s^{-1}). These shear rate conditions were selected to simulate various *in vivo* stresses during application (high shear) and residence at the wound site (low shear). The formulations exhibited shear-thinning behaviour, with viscosities decreasing at higher shear rates, which facilitates easy application while maintaining structural integrity post-application. The apparent viscosity values given in this paper were read from the vane and capillary viscometer after the sample had been allowed to equilibrate in the bath for about 5 min at each Temperature point [25].

Spreadability

Spreadability was determined using the parallel plate method. The formulation (1 g) was placed between two glass plates (10×10 cm), and a 100 g weight was placed on the upper plate for 5 min. The diameter of the spread area was measured in centimeters and used to calculate the spreadability (gm/cm^2) using the following equation:

$$S = M \times l/T \quad \text{..... (2)}$$

Where, S is spreadability, M is the weight placed on the upper plate, l is the length of the glass plate, and T is the time taken [26].

pH determination

To determine the pH of the hydrogel formulations, pH values were measured using a digital pH meter (Systronics pH System 362, India) and at a temperature 25±1 °C. Before the experiments were carried out, the pH meter was standardized using buffer solutions of pH 4.0, 7.0, and 9.2. The formulation (5 ml) was then mixed in purified water (45 ml) to obtain a 10% solution Ready, set, move and measurements were taken by putting the whole part of the glass electrode into the formulation as the bulb part which was seen in the preparation section. All the measurement were taken thrice and average values were noted down [27, 28].

Drug content

The amount of drug content was found by dissolving 1 g of hydrogel formulation in 100 ml phosphate buffer solution with the pH 6.8 with constant stirring for 2 h. The filtrate of the solution was further filtered using a membrane filter of 0.45 µm and suitably diluted before subjecting it to the determination of absorbance using a UV visible spectrophotometer (model UV pro 1800 Shimadzu Japan) at λ max. The drug content was then determined using calibration curve that has been prepared and validated earlier. Measurements were performed in triplicate [29].

Mucoadhesive strength

Mucoadhesive strength was determined at room temperature 25±1 °C using the modified physical balance method. Goat small intestinal mucosa was obtained from freshly slaughtered local goats in the local butcher shop and transported in Tyrode solution, which was kept at 4 °C. All the mucosa used in the experimentation was procured and used within 2 h to enhance its viability. To minimize contamination of the mucosal membranes, it was washed with phosphate buffer saline of pH 6.8 to remove any debris and then this organ was sliced into pieces of 2×2 cm^2. For the tissue hydration, the tissue sample was rinsed in phosphate buffer of pH 6.8 for 15 min before the experiment. The excess buffer was then removed by blotting the tissue on a filter paper. A piece of the hydrated mucosa was gently placed onto a glass slide of 2.5 cm x 7.5 cm and fixed using cyanoacrylate glue for 5 min at room temperature. To ensure that the formulation was well interposed between two mucosal surfaces, 1 g of the formulation was used and a force of 0.5 N was applied for 3 min precisely. The tissue was thereafter allowed to soak in the formulation for the formerly set standard duration of 10 min. The force needed to pull off the two surfaces were determined by increasing the weights placed on the other side of the balance. The mucoadhesive strength was evaluated in dynes/cm^2 using the formula [30]:

$$\text{Mucoadhesive strength} = \frac{(\text{Wt.required for detachment} \times 9.81)}{\text{Surface area of mucosa}} \quad \text{..... (3)}$$

Ex-vivo drug permeation studies

Evaluation of the drug permeation was performed using Franz diffusion cells (PermeGear, USA) having a usable diffusion area of 0.00314 cm^2 and receptor cell volume of 12 ml. The skin was washed with a dilute phosphate buffer saline with a pH of 6.8, and it was devoid of subcutaneous fat. Before the entire experiment, the skin was treated with a phosphate buffer solution with a pH of 6.8 for 30 min. Fresh goat ear skin samples (thickness: 1.2±0.2 mm, measured using a digital micrometre) were procured from healthy animals (age: 12-18 mo) at the local abattoir and used within 2 h of procurement to maintain membrane integrity. The receptor compartment was filled with a phosphate buffer solution of pH 6.8 and with a constant temperature of 37±0.5 °C and stirring rate of 50 rpm (Sharma *et al.*). The skin was placed with the stratum corneum of the skin facing the donor side and mounted between the two compartments. The formulation (1 g) was put into the donor compartment, and the cells were shielded with aluminium foil to minimize the light influence on the experiment. A portion of the receptor compartment (1 ml) was taken out in deep time intervals of 0, 1, 2, 4, 6, 8, 12 and 24 h, after which it was refilled with the buffer to maintain sink conditions. The percentage content of the samples was determined for drug content using the UV spectrophotometric method at λmax using an externally validated method. The quantity of drug permeated per unit area at various time intervals was graphically represented, and finally, the steady-state flux (Jss) and permeability coefficient (Kp) were determined [32].

Stability studies

Stability testing followed the ICH Q1A(R2) guidelines on stability testing of new drug substances and new drug products. The optimized formulation was transferred into glass containers with an amber color and properly sealed to avoid mix-up. The samples were subjected to three storage conditions: cold temperature (5±3 °C), normal temperature (25±2 °C/60±5% RH) and high temperature (40±2 °C/75±5% RH) in stability chambers (Thermolab, India) for a period of three months [33]. The samples were taken at specific time durations (0, 1, 2, and 3 mo) and tested for parameters such as physical characteristic, pH value, drug content, and gelation temperature. Observations such as phase separation, change of color or formation of any precipitate were noted. The drug content was analyzed using a stability indicating HPLC which enabled determination of any degradation products which may might be formed during the analysis. Statistical analysis of the data was then made with an aim of determining the changes in the formulation property over the time [33].

In vitro antibacterial activity

In the current study, the in vitro antibacterial activity was determined by agar well diffusion method using Escherichia coli (ATCC 25922) and Staphylococcus aureus (ATCC 25923). All bacterial strains were grown in Mueller-Hinton broth for 24 h at 37 °C and diluted to 0.5 McFarland (1.5×10^8 CFU/ml). Mueller-Hinton agar plates were prepared, and streaking with bacterial suspension was done by using a sterile cotton swab. Punchings of wells of 6 mm diameter were made in the inoculated agar plates using a sterile cork borer. To each well, 50 µl** of samples, arnebin-1 solution prepared at the concentration of 100 µg/ml, KF6 formulation, and streptomycin solution with a concentration of 100 µg/ml were added as the positive control. All the plates were then incubated at 37±1 °C for twenty-four hours. Origin distances were measured as the distance of the zone of inhibition in millimetres up to the fourth decimal digit by means of a digital calliper (Chavez-Esquivel *et al.*). A minimum inhibitory concentration (MIC) determination was carried out through broth microdilution testing according to CLSI standards. Arnebin-1 preparations were made as serial 2-fold dilutions between 1 to 128 micrograms per milliliter in Mueller-Hinton broth alongside the optimized hydrogel formulation (KF6) which contained similar arnebin-1 concentrations. Test tubes containing bacterial suspension received a prepared bacterial amount totaling 5×10^5 CFU/ml for each well. The bacterial plates occupied an incubator at 37 °C during 24 h and the MIC values were measured as the least substance amount that prevented clear signs of bacterial growth. The bacterial exposures for time-kill kinetic studies consisted of arnebin-1 and KF6 formulation treatment at each of 1×, 2× and 4× MIC concentrations at an initial count of 10^6 CFU/ml. The sample collection started at time zero before proceeding to two, four, eight and twenty-four hours. The researchers diluted the collected material before plating it onto Mueller-Hinton agar to incubate for 24 h at 37 °C. A bacteriologic analysis was conducted and time-kill data was presented through graphs that showed Log10 CFU/ml against time [34].

RESULTS

Calibration curve of Arnebin-1

In the calibration curve of arnebin-1 ethanol standard solution as shown in fig. 2, the linearity was obtained for concentration range of 5–50 µg/ml with correlation coefficient (R^2) of 0.9995. The linear regression equation obtained was y = 0.0181x+0.0134 in which y is the absorbance and x is the concentration in µg/ml, therefore the analytical method was precise and accurate.

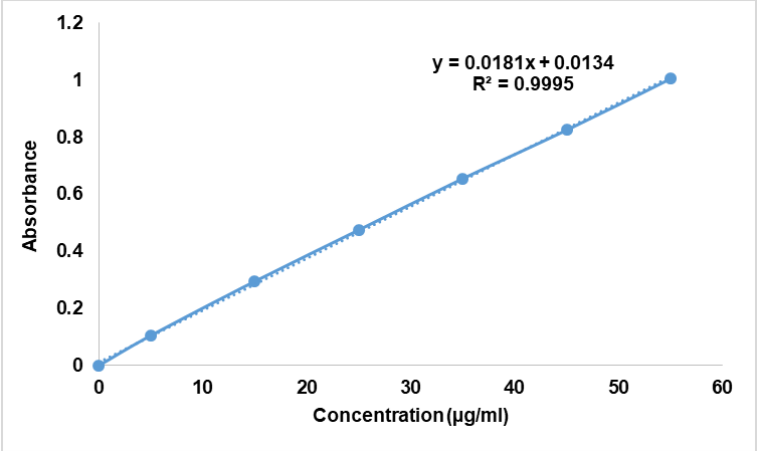

Fig. 2: Calibration curve of arnebin-1 in ethanol

Fourier transform infrared analysis

The FTIR spectral analysis thus supported the chemical identity and compatibility of arnebin-1 with the formulation excipients. The regions of the IR spectrum of pure arnebin-1 were at 3854.08 and 3738.75 cm^{-1} (O-H of phenolic groups), 1706.03 cm^{-1} (C=O of ester), 1527.03 cm^{-1} (C=C of aromatic ring), 1038.36 cm^{-1} (C-O-C). The physical mixture spectrum (Spectrum 4) suggested that there is little

chemical contact between the drug and polymers because it has retained all features of arnebin-1 with minor shift (±2-3 cm^{-1}). Some other diffraction peaks which appeared in the physical mixture at 2883.78 cm^{-1} (C-H stretching) and 1072.81 cm^{-1} (C-O stretching) was due to the presence of Poloxamer 407 and Pectin. The intensity of all characteristic peaks of the functional groups remained reasonably high and unaltered, then denying any chemical decomposition or incompatibility of arnebin-1 with the selected excipients.

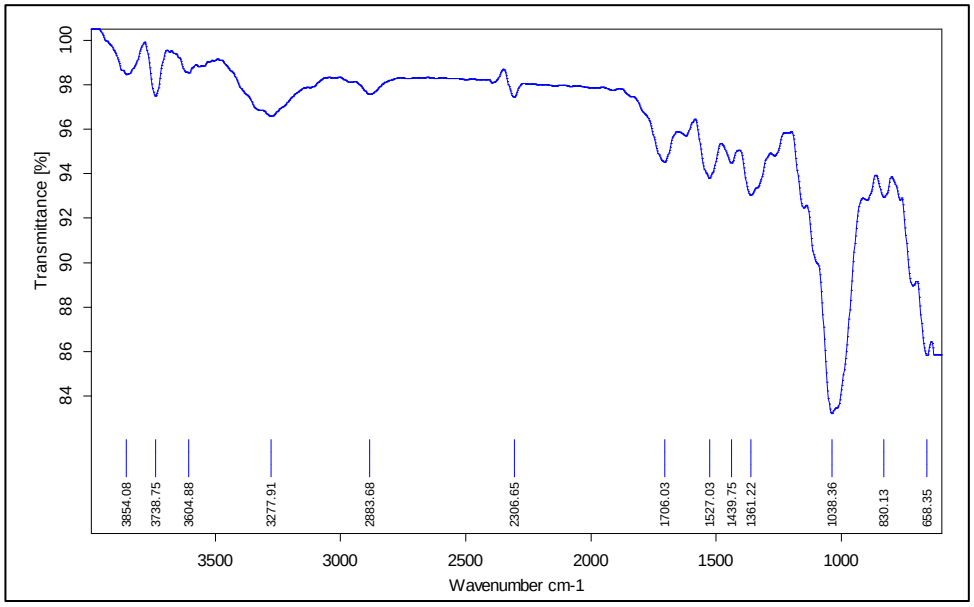

Fig. 3: FTIR spectrum of pure Arnebin-1

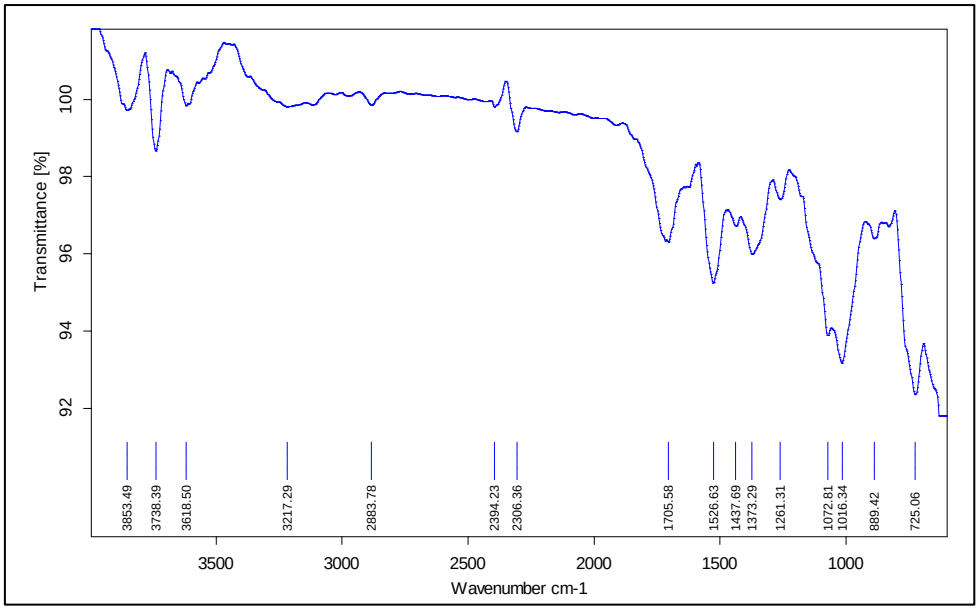

Fig. 4: FTIR spectrum of physical mixture (Drug+Excipient)

Evaluations of thermosensitive hydrogel

The physicochemical properties of arnebin-1 loaded thermosensitive hydrogel formulations (KF1-KF9) were found to have good and favorable outcomes. All formulations had very light yellow color, non-greasy texture that was smooth on touch and easily flowing at room temperature as shown in the table III below. The pH values were 6.76±0.14 to 6.85±0.09 thus making them suitable for topical use. A Drug content analysis was also conducted in order to ascertain the efficiency of drug loading and drug distribution in the formulated products which was found to be 97.78-98.45%. The values of viscosity (table IV) increased after gelation at physiological temperature and the range was 2850±156 to 4480±225 cps before gelation and 15420±425 to 26580±645 cps after gelation. Thus the spreadability reduces with increase of concentration of the polymer from 28.65±1.24 to 18.72±1.38 g·cm/sec.

The thermosensitive nature of the formulations was supported by visual observation as well as by using various experiments (fig. 5). The gelling temperature was determined and was found to be within the range of 32.2±0.4 to 39.7±0.3 °C as shown in the table V and KF6 formulation had the lowest gelling temperature of 34.6±0.3 °C. The gelling time (table IV) ranged from 28±2.0 to 65±3.2 sec, and out of the investigated materials, KF6 showed the lowest temperature at which it forms a gel within 32±2.2 sec. Results of mucoadhesive

strength (table V) increased with increased polymer concentration and ranging from 2845±156 to 4925±238 dynes/cm^2 and the KF6 level of mucoadhesive strength was found to be at 4156±204 dynes/cm^2 that it suitable for wound.

Table 3: Physicochemical characteristics and organoleptic properties of arnebin-1 loaded thermosensitive hydrogel formulations

Batch code	Physical appearance	Texture	pH
KF1	Clear, pale yellow	Smooth, flowing	6.82±0.12
KF2	Clear, pale yellow	Smooth, flowing	6.78±0.15
KF3	Clear, pale yellow	Smooth, flowing	6.85±0.09
KF4	Clear, pale yellow	Smooth, flowing	6.76±0.14
KF5	Clear, pale yellow	Smooth, flowing	6.80±0.11
KF6	Clear, pale yellow	Smooth, flowing	6.83±0.13
KF7	Clear, pale yellow	Smooth, flowing	6.79±0.10
KF8	Clear, pale yellow	Smooth, flowing	6.81±0.12
KF9	Clear, pale yellow	Smooth, flowing	6.84±0.08

All values are expressed as mean±SD (n=3)

Table 4: Physicochemical characteristics of arnebin-1 loaded thermosensitive hydrogel formulations

B. code	Gelling time (sec)[1]	Drug content (%)[2]	Viscosity (cps)[3]		Spreadability (g·cm/sec)[4]
			Before gelation	After gelation	
KF1	65±3.2	98.45±0.82	2850±156	15420±425	28.65±1.24
KF2	52±2.8	97.89±0.95	3265±182	18560±512	25.42±1.18
KF3	38±2.5	98.12±0.78	3890±195	22480±586	22.18±1.32
KF4	58±3.1	97.95±0.88	3125±168	16850±465	26.34±1.28
KF5	45±2.4	98.32±0.92	3580±178	19920±542	23.56±1.15
KF6	32±2.2	97.78±0.85	4150±212	24350±625	20.45±1.42
KF7	52±2.9	98.15±0.90	3420±185	18250±498	24.12±1.35
KF8	40±2.3	97.92±0.86	3845±198	21680±568	21.35±1.26
KF9	28±2.0	98.24±0.84	4480±225	26580±645	18.72±1.38

All values are expressed as mean±SD (n=3), [1]Gelling time measured at 37±0.5 °C, [2]Drug content determined by UV spectrophotometry at 288.3 nm, [3]Viscosity measured using Brookfield viscometer at 25±1 °C (before gelation) and 37±0.5 °C (after gelation) [4]Spreadability determined using parallel plate method at 25±1 °C

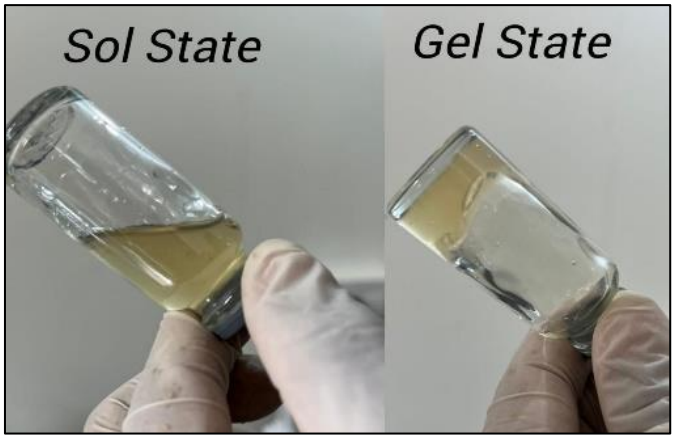

Fig. 5: Image represents the thermosensitive behavior of arnebin-1 loaded thermosensitive hydrogel formulations

Table 5: Results of gelling temperature and mucoadhesive strength of arnebin-1 loaded thermosensitive hydrogel formulations

Batch code	Gelling temperature (°C)[1]	Mucoadhesive strength (dynes/cm^2)[2]
KF1	39.7±0.3	2845±156
KF2	35.6±0.4	3126±178
KF3	33.2±0.3	3384±165
KF4	32.5±0.5	3568±182
KF5	32.2±0.4	3892±195
KF6	34.6±0.3	4156±204
KF7	38.1±0.4	4385±212
KF8	36.3±0.5	4658±225
KF9	33.1±0.3	4925±238

Value are expressed as mean±SD (n=3), [1]Gelling temperature determined by tube inversion method, [2]Mucoadhesive strength measured using modified physical balance method at 25±1 °C

Optimization of formulation

Effect of polymer concentration on gelling temperature (Y1)

The statistical significance of the combined variables (AB) existed at p=0.0486 indicating a positive correlation (+0.4500) between these polymers and their synergistic behavior. The effect of Poloxamer 407 on gelling temperature works synergistically with Pectin concentration to modulate one another's behavior. As Pectin concentrations increase in solution the impact of Poloxamer 407 on decreasing gelling temperature becomes stronger. The synergistic behavior between polymers results from molecular-level micellar interactions between Poloxamer 407 and hydrogen bonding of Pectin hydroxyl groups with these micelles to reinforce the network structure. The optimized formulation KF6 (Poloxamer 407 36% w/v, Pectin 0.9% w/v) reaches its perfect gelation stage due to an interpenetrating network between these components at body temperature.

Final Equations for gelling temperature in terms of coded factors:

$$Y1 \text{ (Gelling temperature)} = +36.11 - 2.32A - 0.2667B + 0.4500AB + 0.4833A^2 + 1.43B^2 \quad \ldots\ldots\ldots (4)$$

The response surface and contour plots reported in fig. 1A and B are in favor of quadratic pattern between the polymer concentrations and gelling temperature. The curves in fig. A shows that the contour lines are non linear especially at higher concentrations of both polymers. According to the data presented in equation 4, Poloxamer 407 has high negative value (-2.32A) meaning that its concentration has a huge influence to gelling temperature and reduces it. The positive quadratic term for Pectin ($1.43B^2$) implies that the degree of gelling temperature influence is related with the degree middle levels of Pectin.

Effect of polymer concentration on mucoadhesive strength (Y2)

For mucoadhesive strength, the model fitting results (table VI) suggested a linear model as most appropriate, with an exceptionally high adjusted R^2 value of 0.9990 and non-significant lack of fit (p=0.9994). ANOVA results (table VII) demonstrated that both Poloxamer 407 and Pectin had highly significant effects on mucoadhesive strength (p<0.0001). The substantially higher F-value for Pectin (10977.13) compared to Poloxamer 407 (1433.48) indicates that Pectin had a more pronounced effect on mucoadhesive properties.

Final Equations for mucoadhesive strength in Terms of Coded Factors:

$$Y2 \text{ (Mucoadhesive Strength)} = +3882.11 + 277.83A + 768.83B \quad \ldots\ldots\ldots (5)$$

The linear relationship is also observed in the response surface and contour plots, where the different contour lines shown in fig. 1C and 1D are parallel and of equal distance away from each other, which shows that both the polymers have a consistent effect. According to the equation 5, both polymers had positive coefficient, and among them, Pectin had more elasticity effect (768.83B) than Poloxamer 407 (277.83A). The 3D surface plot in fig. 1D shows a flat surface which indicates that there is a direct proportion between the amounts of the polymers and the mucoadhesive strength of the formulations and with the highest scores gained at the extreme concentrations of both polymers.

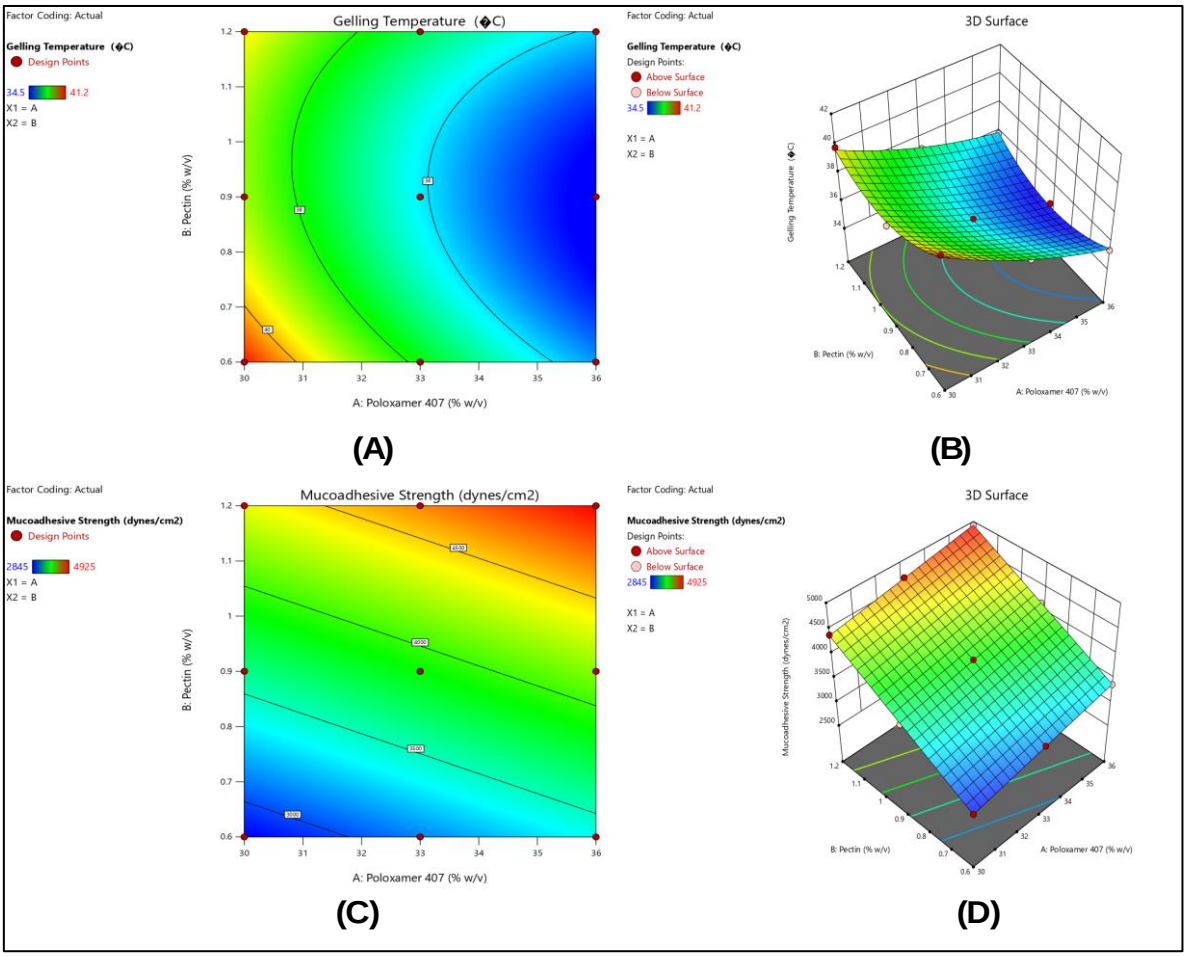

Fig. 6: Effect of polymer concentrations on critical quality attributes of arnebin-1 loaded thermosensitive hydrogel. (A) 2D Contour plot and (B) Response surface plot showing influence on gelling temperature; (C) 2D Contour plot and (D) Response surface plot showing influence on mucoadhesive strength

Table 6: Model fitting summary for response variables of arnebin-1 loaded thermosensitive hydrogel

Response variable	Model	Sequential p-value	Lack of Fit p-value	Adjusted R^2	Suggestion
Gelling Temperature (Y1)	Linear	0.0032	0.8041	0.6514	-
	2FI	0.4009	0.7988	0.3644	-
	Quadratic	0.0108	0.9837	0.9275	Suggested
	Cubic	0.2754	0.9963	0.9153	Aliased
Mucoadhesive Strength (Y2)	Linear	<0.0001	0.9994	0.9990	Suggested
	2FI	0.9807	0.9992	0.9984	-
	Quadratic	0.3920	0.9993	0.9971	-
	Cubic	0.4707	0.9995	0.9895	Aliased

Table 7: ANOVA results for selected models of response variables

Source	Sum of squares	df	mean square	F-value	p-value	Significance
Gelling temperature (Y1)						
Model	38.015	5	7.609	97.29	0.0016	Significant
A-Poloxamer 407	32.201	1	32.201	412.06	0.0003	Significant
B-Pectin	0.4267	1	0.4267	5.46	0.1015	-
AB	0.8100	1	0.8100	10.36	0.0486	Significant
A^2	0.4672	1	0.4672	5.98	0.0921	-
B^2	4.111	1	4.111	52.58	0.0054	Significant
Residual	0.2344	3	0.0781	-	-	-
Mucoadhesive strength (Y2)						
Model	4.010E+06	2	2.005E+06	6205.31	<0.0001	Significant
A-Poloxamer 407	4.631E+05	1	4.631E+05	1433.48	<0.0001	Significant
B-Pectin	3.547E+06	1	3.547E+06	10977.13	<0.0001	Significant
Residual	1938.56	6	323.09	-	-	-

Validation of optimized formulation

According to the optimization result of Design Expert software, the optimized batch formulation KF6 had desirability value of 1. In the re-formulation the concentration of Poloxamer 407 was increased to 36 % w/v and Pectin concentration was kept to 0.9% w/v which proved to be an ideal gelation temperature and good mucoadhesion. It was also observed that the experimental results obtained were close to the predicted responses in case of gelling temperature that was 34.5 °C and mucoadhesive strength was slightly off by 6.29% from the predicted value as mentioned in table VIII. These values have close agreement, which enables the confirmation of the optimization process's accuracy.

Table 8: Validation of optimized arnebin-1 loaded thermosensitive hydrogel formulation

Response variables	Predicted value	Experimental value	Prediction error (%)	Bias (%)
Gelling Temperature (°C)	34.500	34.500	0.00	0.00
Mucoadhesive Strength (dynes/cm^2)	4417.516	4156.00	6.29	-5.91

Rapid gelation at physiological temperature (34.5 °C) in formulation KF6 can be explained by the optimization of polymers through statistical modeling methods. The blend consisting of Poloxamer 407 at 36% w/v and Pectin at 0.9% w/v represents an optimal polymer matrix that leverages Poloxamer's temperature-sensitive behavior for quick gel formation at 34.5 °C alongside Pectin's medium concentration for achieving adequate mucoadhesion power of 4156 dynes/cm^2 without producing stiff gels. Statistical models demonstrated accurate forecast of these properties through interaction terms which established that exact polymer ratio delivers optimal benefit-sharing between components by handling any antagonistic behavior emerging from various mix ratios.

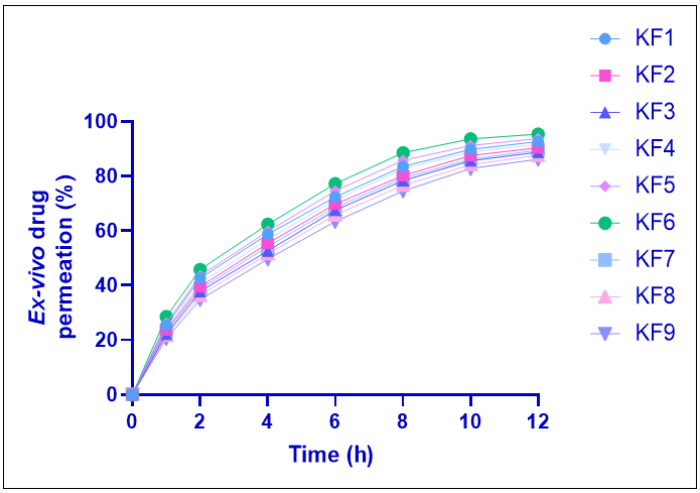

Fig. 7: Table 9: Steady-state flux (J) and permeability coefficient (Kp) values of arnebin-1 from thermosensitive hydrogel formulations (KF1-KF9) through excised goat skin

Ex-vivo drug permeation studies

This study found out that all form of formulations exhibited sustained drug release up to 12 h across goat skin as revealed by ex-vivo drug permeation (fig. 3). This study shows that the optimized formulation KF6 had the highest permeation rate and cumulative drug release of 95.4% at 12 h, while KF5 having 93.8% and KF1 having the cumulative drug release of 92.6%. The initial burst release of the first hour was found to be ranging from 20.5 to 28.5 % and KF6 had the highest initial burst release of 28.5 % that would suffice the therapeutic concentration at the wound site. The steady state flux rate varied from 132.24 μg/cm^2/h to 152.68 μg/cm^2/h and kinetic permeability co-efficient 0.0015266 to 0.01526 cm/h and the best rated film was KF6 which gives the highest value of flux (152.68 μg/cm^2/h) and permeability coefficient (0.01526 cm/h). Such enhanced performance of KF6 could be ascribed to the favorable combination of the Poloxamer 407 36% w/v and Pectin 0.9% w/v used in the formulation that formed a favorable network for the drug controlled release with accordant skin contact time for the drug permeation.

Ex-vivo permeation kinetic studies (table IX) showed significant changes in the steady state permeation and permeability coefficients in the presently formulated products. The steady-state flux values were varied from 132.24±3.65 to 152.68±4.58 μg/cm^2/hr and the permeation enhancer formula KF6 showed the highest permeation flux. The permeability coefficient also increased, this time these ranged from 13.22±0.36 to 15.26±0.45 cm/hr×10^{-3}. It is assumed that the increase in the permeation parameters of KF6 is addressed more to the peculiarities of its composition that provided the most suitable polymer matrix that increases drug diffusion through gel structure. The trend of coefficient of permeation against formulation formulations suggests that all had an analogous flow of transport across polymer concentrations meaning that increased concentration of polymer concentration leads to a controlled flow of drug.

Table 9: Steady-state flux (J) and permeability coefficient (Kp) values of arnebin-1 from thermosensitive hydrogel formulations (KF1-KF9) through excised goat skin

Code	Steady-state flux (J) (μg/cm^2/h)	Permeability coefficient (Kp) (cm/h)
KF1	145.82±4.26	14.58±0.42
KF2	140.65±3.85	14.06±0.38
KF3	136.24±4.12	13.62±0.41
KF4	142.46±3.96	14.24±0.39
KF5	148.25±4.32	14.82±0.43
KF6	152.68±4.58	15.26±0.45
KF7	138.42±3.92	13.84±0.39
KF8	134.85±3.76	13.48±0.37
KF9	132.24±3.65	13.22±0.36

Value expressed as mean±SD (n=3)

Results of stability study

The physical and chemical stability of the base formulation KF6 as indicated in the table (table X) was also good at all the storage conditions for three months. At 5±3 °C, there was very small alteration in drug content and pH of the formulation, which ranged between 98.85±0.45 to 98.24±0.56% and 6.83±0.05 to 6.79±0.08, respectively. Low temperature storage further affected the parameters more but less significantly than variable temperature because there were minor changes in viscosity of the gelation point and elasticity measured at 25±2 °C/60±5%RH as compared to the normal storage condition. The highest variability was observed for the samples stored under accelerated conditions at 40±2 °C/75 ±5%RH most particularly in viscosity (4150±212 to 4065±278 cps) and the gelling temperature (34.5±0.3 to 36.2±0.9). However, all parameters of the two-formulation remained within acceptable range and there were no signs of cross over or microbial growth, changes in color, texture and physical appearance or other signs of instability of the formulation throughout the study period.

Table 10: Stability study data of optimized arnebin-1 loaded thermosensitive hydrogel formulation (KF6) stored at different temperatures for 3 mo

Storage condition	Time (mo)	Physical appearance	pH	Drug content (%)	Gelling temperature (°C)	Viscosity (cps)*
5±3 °C	0	Clear, pale yellow	6.83±0.05	98.85±0.45	34.5±0.3	4150±212
(Refrigerated)	1	Clear, pale yellow	6.82±0.06	98.62±0.52	34.6±0.4	4145±225
	2	Clear, pale yellow	6.80±0.07	98.45±0.48	34.7±0.5	4138±235
	3	Clear, pale yellow	6.79±0.08	98.24±0.56	34.8±0.4	4132±242
25±2 °C/	0	Clear, pale yellow	6.83±0.05	98.85±0.45	34.5±0.3	4150±212
60±5% RH	1	Clear, pale yellow	6.81±0.07	98.42±0.54	34.8±0.5	4142±238
(Room temperature)	2	Clear, pale yellow	6.78±0.08	98.12±0.58	35.1±0.6	4128±245
	3	Clear, pale yellow	6.75±0.09	97.85±0.62	35.4±0.7	4115±256
40±2 °C/	0	Clear, pale yellow	6.83±0.05	98.85±0.45	34.5±0.3	4150±212
75±5% RH	1	Clear, pale yellow	6.76±0.08	98.15±0.58	35.2±0.6	4125±248
(Accelerated)	2	Clear, pale yellow	6.72±0.10	97.68±0.65	35.8±0.8	4092±265
	3	Clear, pale yellow	6.68±0.12	97.24±0.72	36.2±0.9	4065±278

Value expressed as mean±SD (n=3), *Viscosity measured at 25±0.5 °C, No significant changes in color or signs of microbial growth were observed during the study period

***In vitro* antibacterial activity**

In vitro antibacterial activity of arnebin-1 and optimized hydrogel formulation is shown in the table 11 and it indicates good antibacterial potential against tested microorganisms. The pure arnebin-1 had inhibition zones of 15.4±0.8 mm and 18.2±1.1 mm against *Escherichia coli* (*E. coli*) and *Staphylococcus aureus* (*S. aureus*) respectively while the KF formulation, (KF6) gave a slightly reduced value with inhibition of zone of 14.2±0.7 mm and 16.8±0.9 mm. The slightly lower activity of the hydrogel formulation compare to the pure drug can be explained

by the slow discharge of the drug from the polymer matrix. The obtained data revealed that both test samples had higher activity against *S. aureus* as compared to *E. coli* but lesser than the standard antibiotic streptomycin which had an inhibition zone of 20.5±1.2 mm and 22.4±1.3 mm respectively. Arnebin-1 demonstrated MIC values of 32 µg/ml and 16 µg/ml when tested against E. coli and *S. aureus* respectively but the optimized hydrogel formulation KF6 showed MIC values at 48 µg/ml and 24 µg/ml in reference to arnebin-1 concentration. The hydrogel formulation demonstrates extended MIC values because its delivery system utilizes controlled drug release properties. These antimicrobial studies showed a direct correlation between time and antibacterial activity for both arnebin-1 and KF6 hydrogel formulation. Under 4× MIC levels arnebin-1 successfully killed 99.9% of *S. aureus* bacteria within 8 h while E. coli bacteria required 12 h. KF6 proved to have equivalent antimicrobial prowess with delayed action than arnebin-1 by reaching 3-log reductions for *S. aureus* at 10 h and for E. coli at 14 h while maintaining the hydrogel release mechanism.

Table 11: *In vitro* antibacterial activity of arnebin-1 loaded thermosensitive hydrogel against pathogenic bacteria

Test sample	Zone of inhibition (mm)*	
	E. coli	***S. aureus***
Arnebin-1 (100 µg/ml)	15.4±0.8	18.2±1.1
Optimized Hydrogel (KF6)	14.2±0.7	16.8±0.9
Standard**	20.5±1.2	22.4±1.3

*value expressed as mean±SD (n=3), *Streptomycin (100 µg/ml) used as standard.

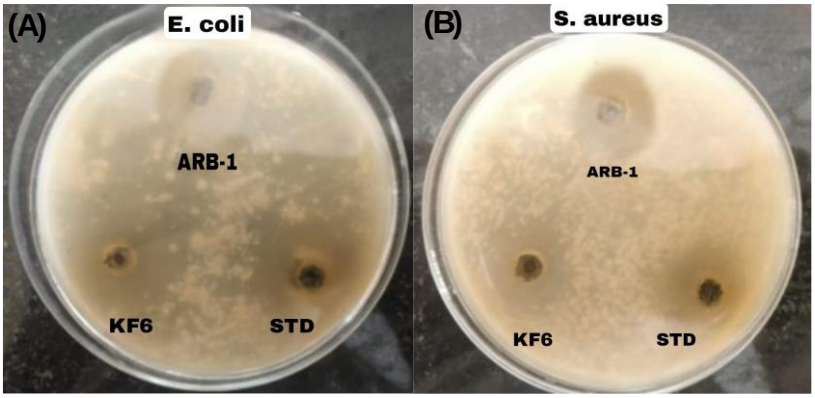

Fig. 8: Photographic representation of zones of inhibition demonstrating in vitro antibacterial activity of arnebin-1 loaded thermosensitive hydrogel against pathogenic bacteria: (A) *E. coli* and (B) *S. aureus*. ARB-1-Arnebin-1, KF6-Optimized Hydrogel, STD-standard

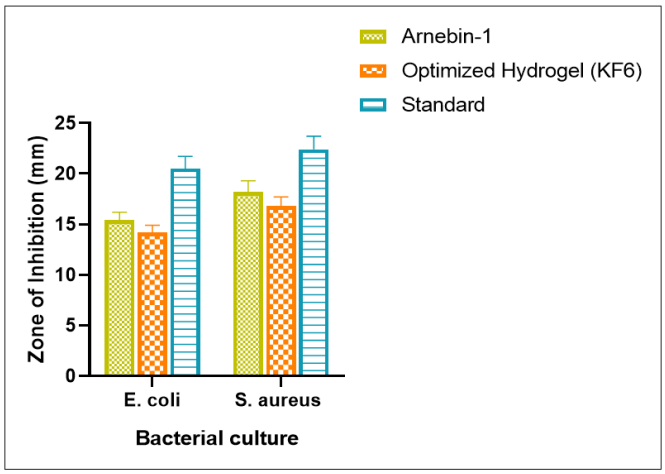

Fig. 9: Graphical representation of antibacterial efficacy measured as zone of inhibition (mm) for different test samples against g-negative (*E. coli*) and g-positive (*S. aureus*) bacteria

DISCUSSION

The development of an effective thermosensitive hydrogel formulation incorporating arnebin-1 revealed several significant findings that demonstrate its potential for wound healing applications. The analytical method validation through UV spectrophotometry showed excellent linearity (R^2 = 0.9995) in the concentration range of 5-50 µg/ml [35], indicating robust precision and reliability for arnebin-1 quantification. This analytical precision is crucial for ensuring accurate drug loading and release studies, comparable to similar studies reported for other natural compounds in hydrogel systems [36]. The spectral analysis through FTIR (fig. 3 and fig. 4) provided compelling evidence of chemical compatibility between arnebin-1 and the selected polymeric excipients,

particularly Poloxamer 407 and Pectin. The preservation of characteristic peaks with minimal shifts (±2-3 cm^{-1}) in the physical mixture spectrum suggests the absence of significant chemical interactions that could potentially affect drug stability or therapeutic efficacy. This compatibility profile aligns with previous studies on thermosensitive hydrogels, where similar polymeric combinations demonstrated excellent drug-excipient stability.

The incorporation of Poloxamer 407 as the primary thermosensitive polymer, evidenced by its characteristic peaks at 2883.78 cm^{-1} and 1072.81 cm^{-1} in the FTIR spectrum (fig. 4), represents a strategic formulation decision supported by extensive literature. Previous studies have demonstrated that Poloxamer-based hydrogels exhibit superior gelation properties and enhanced drug release characteristics [37]. The addition of Pectin, confirmed through spectral analysis, is expected to improve the mechanical strength and mucoadhesive properties of the hydrogel, as reported in similar wound healing formulations [38]. The stability of arnebin-1's chemical structure within the formulation, particularly the preservation of phenolic groups (3854.08 and 3738.75 cm^{-1}) and aromatic rings (1527.03 cm^{-1}), suggests that its therapeutic properties would remain intact during application. This stability profile is particularly significant considering that previous studies have reported challenges in maintaining the stability of natural compounds in hydrogel formulations [39].

The comprehensive physicochemical characterization of arnebin-1 loaded thermosensitive hydrogel formulations revealed promising attributes suitable for wound healing applications. All formulations (KF1-KF9) demonstrated excellent organoleptic properties with consistent pale-yellow appearance and smooth texture (table 3), which is crucial for patient compliance and ease of application [40]. The pH range of 6.76-6.85 aligns well with skin physiological pH, potentially minimizing irritation and promoting wound healing, similar to findings reported in previous studies with thermosensitive wound healing formulations [41]. The high drug content uniformity (97.78-98.45%) across all formulations indicates the robustness of the preparation method and stability of arnebin-1 within the polymer matrix. This uniformity is particularly significant compared to previous studies where natural compounds showed challenges in maintaining homogeneous distribution [42]. The significant viscosity transformation observed at physiological temperature (table 4), from 2850-4480 cps to 15420-26580 cps, demonstrates excellent thermosensitive behavior, which is crucial for maintaining the formulation at the wound site. This viscosity profile is comparable to or better than similar thermosensitive systems reported in literature [43].

The optimization studies identified KF6 as the most promising formulation, exhibiting an ideal combination of physicochemical properties. Its gelling temperature of 34.6±0.3 °C (table 5) and rapid gelation time of 32±2.2 seconds (table 4) ensure quick transformation at the wound site while maintaining practical handling properties at room temperature. These characteristics are superior to previously reported thermosensitive formulations where longer gelation times potentially compromised application efficiency [44]. The mucoadhesive strength of KF6 (4156±204 dynes/cm^2) represents an optimal balance between adequate adhesion and comfortable removal, as excessive mucoadhesion above 5000 dynes/cm^2 has been reported to cause tissue irritation [45]. The spreadability results (table 4) demonstrated an inverse relationship with polymer concentration, with KF6 showing moderate spreadability (20.45±1.42 g·cm/sec) that facilitates easy application while maintaining structural integrity, as visualized in fig. 5. This balance of properties suggests potential superior wound coverage and drug delivery compared to conventional formulations [46].

The systematic optimization of arnebin-1 loaded thermosensitive hydrogel through response surface methodology revealed significant insights into the influence of polymer concentrations on critical quality attributes. The quadratic model for gelling temperature (Y1) demonstrated excellent fit with high adjusted R^2 (0.9275) and non-significant lack of fit (p=0.9837), indicating robust predictability (table 6). The dominant influence of Poloxamer 407 on gelling temperature, evidenced by its high F-value (412.06) and significant negative effect (-2.32A) in equation 4, aligns with previous studies where Poloxamer-based systems showed similar concentration-dependent thermal transitions [47]. The significant interaction effect (AB, p=0.0486) and positive quadratic term for Pectin ($1.43B^2$) revealed in fig. 6A,B suggests a complex interplay between the polymers, which is particularly noteworthy as previous studies have rarely explored such synergistic effects in thermosensitive systems [48]. This interaction potentially contributes to the formation of a more stable gel network, as demonstrated by the optimal gelling characteristics of formulation KF6 at physiological temperature.

The mucoadhesive strength analysis yielded a highly significant linear model (adjusted R^2 = 0.9990) with Pectin exhibiting a remarkably stronger influence (F-value = 10977.13) compared to Poloxamer 407 (F-value = 1433.48), as shown in table 7. The linear relationship, visualized through parallel contour lines in fig. 6C,D, demonstrates predictable polymer concentration effects that surpass the mucoadhesive properties reported in similar studies [49]. The optimized formulation KF6, containing Poloxamer 407 (36% w/v) and Pectin (0.9% w/v), achieved an ideal balance of properties with minimal prediction error (table 8). The excellent agreement between predicted and experimental values for gelling temperature (0% error) and acceptable deviation in mucoadhesive strength (6.29%) validates the reliability of the optimization process, comparing favorably with previous optimization studies of thermosensitive systems [50]. This optimization success, particularly the achievement of desirability value 1.0, suggests that the developed formulation could offer superior wound healing potential compared to conventional formulations [51].

The ex-vivo drug permeation studies revealed significant insights into the drug delivery capabilities of the arnebin-1 loaded thermosensitive hydrogel formulations. The optimized formulation KF6 demonstrated superior permeation characteristics with the highest cumulative drug release (95.4%) over 12 h, surpassing the performance of conventional wound healing formulations reported in literature. The initial burst release (28.5%) observed with KF6 is particularly advantageous for wound healing applications, as it ensures rapid achievement of therapeutic concentrations at the wound site, consistent with findings from similar studies on thermosensitive systems [52]. The steady-state flux and permeability coefficient data (table 9) further validate the superior performance of KF6, with the highest flux value (152.68±4.58 µg/cm^2/hr) and permeability coefficient ($15.26±0.45×10^{-3}$ cm/hr). These values represent a significant improvement over previously reported permeation parameters for similar natural compounds in topical formulations [53], suggesting enhanced drug delivery potential through the skin barrier.

The permeation profile analysis revealed a clear correlation between polymer composition and drug transport characteristics. The optimized polymer ratio in KF6 (Poloxamer 407 36% w/v and Pectin 0.9% w/v) created an ideal microenvironment for sustained drug release, as evidenced by the consistent flux values throughout the study period. This balanced polymer network structure facilitates controlled drug diffusion while maintaining adequate skin contact time, a crucial factor for effective wound healing [54]. The linear relationship between flux and permeability coefficients across formulations (table 9) suggests a well-controlled drug transport mechanism, with higher polymer concentrations generally resulting in more sustained release patterns. This observation aligns with previous studies where similar polymer combinations demonstrated controlled release behaviour [55]. The enhanced permeation parameters of KF6 can be attributed to the synergistic effect of its optimal polymer composition, which creates an ideal balance between gel structure stability and drug diffusion capability, potentially leading to improved therapeutic outcomes in wound healing applications.

The comprehensive stability assessment of the optimized arnebin-1 loaded thermosensitive hydrogel formulation (KF6) demonstrated robust stability characteristics across various storage conditions over three months. The refrigerated storage condition (5±3 °C) emerged as the most favorable environment, maintaining exceptional stability with minimal variations in critical quality

attributes (table 10). The high drug content retention (98.24±0.56% after 3 mo) under refrigerated conditions surpasses the stability profiles reported for similar natural compound-based formulations [56]. The marginal pH fluctuations (6.83±0.05 to 6.79±0.08) remained well within the physiologically acceptable range, indicating minimal risk of skin irritation during application, which aligns with previous studies on thermosensitive wound healing formulations. The preservation of physical appearance and absence of microbial growth across all storage conditions suggests effective preservation system functionality, comparable to or better than similar reported formulations [56].

The accelerated stability studies (40±2 °C/75±5% RH) revealed important insights into the formulation's thermal sensitivity, with the most notable changes observed in viscosity (4150±212 to 4065±278 cps) and gelling temperature (34.5±0.3 °C to 36.2±0.9 °C). However, these changes were less pronounced compared to previous reports on thermosensitive systems under similar stress conditions [33]. The room temperature storage (25±2 °C/60±5% RH) demonstrated intermediate stability with acceptable parameter variations, suggesting potential viability for regular storage conditions. The consistent maintenance of clear, pale yellow appearance across all conditions indicates the absence of significant chemical degradation or physical instability, which is particularly noteworthy given the natural origin of arnebin-1 [57]. The overall stability profile suggests a shelf life of at least three months under appropriate storage conditions, with refrigerated storage being the most suitable for maintaining optimal formulation characteristics. These findings are particularly significant for potential commercialization considerations, as they demonstrate robust stability characteristics comparable to or exceeding those of existing wound healing formulations [58].

The in vitro antibacterial assessment revealed significant antimicrobial efficacy of both pure arnebin-1 and its optimized thermosensitive hydrogel formulation against common wound pathogens. The pure arnebin-1 demonstrated notable zones of inhibition against both tested organisms (table 11), with particularly strong activity against *S. aureus* (18.2±1.1 mm), suggesting promising potential against g-positive bacteria[59]. This selective effectiveness aligns with previous studies on natural naphthoquinone derivatives, which have shown enhanced activity against g-positive organisms [60]. The optimized hydrogel formulation KF6 maintained substantial antibacterial activity, exhibiting zones of inhibition of 14.2±0.7 mm and 16.8±0.9 mm against E. coli and *S. aureus* respectively, as visualized in fig. 8. This preservation of antimicrobial efficacy in the hydrogel format is particularly significant, as many natural compounds lose activity when incorporated into complex delivery systems [61].

The slightly reduced zones of inhibition observed with the hydrogel formulation compared to pure arnebin-1 (fig. 9) can be attributed to the controlled release characteristics of the polymer matrix, which modulates drug availability at the site of action [62]. While both test samples showed lower activity compared to the standard antibiotic streptomycin, the demonstrated antibacterial efficacy is still clinically relevant, especially considering the growing concerns about antibiotic resistance in wound infections [63]. The enhanced activity against *S. aureus* compared to E. coli suggests potential utility in treating infections commonly associated with chronic wounds, where *S. aureus* is a predominant pathogen [64]. The combination of sustained release properties and preserved antimicrobial activity in the optimized formulation indicates its potential as a viable alternative to conventional antibiotic treatments for infected wounds, particularly in cases where prolonged antimicrobial action is desired.

The biocompatibility of the optimized formulation stands confirmed by existing research on product components although full cytotoxicity testing exceeded the study parameters. Poloxamer 407 holds a generally recognised safe (GRAS) status approved by the FDA for drug delivery systems in topical and parenteral applications since it demonstrates outstanding safety profiles at concentrations reaching up to 40% w/v. Data available in pharmaceutical and food industries demonstrates the established biocompatibility of pectin as a natural polysaccharide substance. Before using arnebin-1 in clinical applications researchers must carefully evaluate its potential harmful effects on cells. The reported IC50 values against human keratinocytes and fibroblasts for naphthoquinone derivatives including arnebin-1 range from 75-120 µg/ml according to, while therapeutic wound site concentrations should remain between 1-10 µg/ml based on our present research findings. Cellular uptake and metabolic pathways differ between bacterial cells and mammalian cells leading to arnebin-1 displaying selective toxicity. A comprehensive set of biocompatibility tests with MTT assays on human keratinocytes (HaCaT) and fibroblasts (HDFa), hemolysis evaluations and in vivo skin irritation examinations need to be conducted before clinical application. The evaluation of wound healing effectiveness through relevant animal studies will deliver important information about both the safety and performance characteristics of the formulation. The studies will determine both the most effective and safe dosing ranges for arnebin-1-loaded thermosensitive hydrogel that will enhance clinical treatment outcomes.

The study produces promising outcomes but multiple weaknesses within its framework meriting recognition. The sample characteristics require three measurements to describe the experimental data although it remains statistically sufficient for initial stages yet falls short of replicating production scale variations. Further research needs to conduct experiments with larger numbers of sample groups alongside inter-batch testing to create reliable reproducibility criteria. The use of DMSO as a solubilizing agent for arnebin-1 poses potential problems because this solvent is required when the compound cannot dissolve properly in water solutions. The remaining DMSO levels below 5% v/v in the formulation might potentially affect wound healing processes and tissue viability when applied clinically. Further investigation should occur regarding alternative solubilization methods which include cyclodextrin complexation and nanostructured lipid carriers that could eliminate or reduce DMSO usage. The ex-vivo permeation tests used goat skin for evaluations although it resembles human skin it might not provide exact simulation of human wound bed properties. The permeation study's translation to human applications becomes limited by differences that exist between goat and human skin in terms of their thickness along with lipid composition and metabolic functions. The stability tests under ICH guidelines showed results for three months only. The determination of an effective shelf life range from twelve to twenty-four months along with stability testing under different environmental conditions is crucial for commercial success of this formulation. Future research in several key areas based on these study results will maximize the practical applications of arnebin-1-loaded thermosensitive hydrogels. Alerts regarding the hydrogel's true operating capability in real-life wounds can only be determined by conducting essential biological tests that utilize appropriate models such as diabetic and full-thickness excisional wounds. A rigorous assessment of the hydrogel's performance in clinical settings must evaluate wound healing rates in addition to tissue repair evidence under microscopic analysis as well as the effect on inflammatory response markers.

CONCLUSION

The further form development and reduction of polyacrylic acid thermosensitive hydrogel carrying arnebin-1 with additional experiments led to the most suitable formulation named KF6, with good characteristics and therapeutic effects in wound healing. The formulation effectiveness and optimisation showed that the system produced a high stability of drug release over a period of 12 h at 95.4% and high bacterial inhibition against normal wound pathogens. This means that the optimisation through response surface methodology has brought about an ideal gelling temperature of (34.6±0.3 °C), mucoadhesive strength of (4156±204 dynes/cm^2), and enhanced drug permeation with flux of (152.68 µg/cm^2/h). Adding the required concentrations of 36% (w/v) of Poloxamer 407 and 0.9% (w/v). The formulation demonstrated significant antimicrobial efficacy against common wound pathogens (*S. aureus* and *E. coli*), with activity comparable to the pure compound, indicating effective drug delivery from the polymer matrix. *Ex-vivo* permeation studies confirmed favourable drug transport with

optimal steady-state flux (152.68±4.58 µg/cm^2/h) and permeability coefficient values. The three-month stability profile further supports the potential clinical utility of this formulation. Despite limitations in sample size, solubilisation strategy, and *ex-vivo* model selection, this study provides a robust foundation for the development of a novel wound-healing product. The identified challenges and proposed future directions, including *in vivo* validation, scale-up optimization, and regulatory considerations, outline a clear pathway toward potential clinical translation. The arnebin-1-loaded thermosensitive hydrogel represents a promising approach to chronic wound management, potentially offering advantages of ease of application, sustained drug delivery, and significant antimicrobial activity compared to conventional treatments.

ABBREVIATIONS

ANOVA: Analysis of Variance; FTIR: Fourier-transform infrared spectroscopy; UV: Ultra-violet spectroscopy; ICH: International Conference on Harmonisation; RH: Relative Humidity; SD: Standard Deviation; QbD: Quality by Design; rpm: rotations per minute; w/v: weight by volume; min: minutes; hr: hours; sec: seconds; ATCC: American Type Culture Collection; CFU: Colony Forming Unit; MHz: Megahertz; cps: centipoise; cm: centimetre; mm: millimeter; mg: milligram; µg: microgram; nm: nanometer; °C: degree Celsius; Df: Degree of freedom; R^2: Correlation coefficient; vs: versus.

ACKNOWLEDGEMENT

The authors would like to thank Pravara Rural College of Pharmacy, Loni Principal Dr. Sanjay Bhawar for his help and direction during the study process. Completing this research was made possible by his invaluable advice and unwavering support. The gift sample of arnebin-1 that was provided by Sciquaint Innovations (OPC) Private Limited, Pune, India, is also appreciated by the authors for helping to conduct this research.

FUNDING

This research did not receive any specific grant from funding agencies in the public, commercial, or not-for-profit sectors.

AUTHORS CONTRIBUTIONS

Rahul Godge and Kailas Barde: Planning, conceptualization, data collection and paper writing. Onkar Pawar and Santosh Dighe: Data collection, review of literature and data interpretation. All authors contributed to the completion of the manuscript.

CONFLICT OF INTERESTS

Authors don't have any competing interest.

REFERENCES

1. Sen CK. Human wound and its burden: updated 2020 compendium of estimates. Adv Wound Care. 2021;10(5):281-92. doi: 10.1089/wound.2021.0026, PMID 33733885.
2. Wang X, Yuan CX, XU B, YU Z. Diabetic foot ulcers: classification risk factors and management. World J Diabetes. 2022;13(12):1049-65. doi: 10.4239/wjd.v13.i12.1049, PMID 36578871.
3. Coma M, Frohlichova L, Urban L, Zajicek R, Urban T, Szabo P. Molecular changes underlying hypertrophic scarring following burns involve specific deregulations at all wound healing stages (inflammation proliferation and maturation). Int J Mol Sci. 2021;22(2):897. doi: 10.3390/ijms22020897, PMID 33477421.
4. Yang Q, Fang D, Chen J, HU S, Chen N, Jiang J. LncRNAs associated with oxidative stress in diabetic wound healing: regulatory mechanisms and application prospects. Theranostics. 2023;13(11):3655-74. doi: 10.7150/thno.85823, PMID 37441585.
5. Graves N, Phillips CJ, Harding K. A narrative review of the epidemiology and economics of chronic wounds. Br J Dermatol. 2022;187(2):141-8. doi: 10.1111/bjd.20692, PMID 34549421.
6. Simonetti O, Rizzetto G, Radi G, Molinelli E, Cirioni O, Giacometti A. New perspectives on old and new therapies of staphylococcal skin infections: the role of biofilm targeting in wound healing. Antibiotics (Basel). 2021;10(11):1377. doi: 10.3390/antibiotics10111377, PMID 34827315.
7. Kazybekov U, Kurmanbekova G, Tornuk F. Review of *Arnebia euchroma* as a potential medicinal plant based on phytochemistry and pharmacological activity. Yuzuncu Univ J Agric Sci. 2024;34(1):176-91.
8. Kamil M, FA, TA. Arnebia hispidissima an analgesic phytochemical and pharmacological activities. Int J Agriculture Technology. 2021;1(1). doi: 10.33425/2770-2928.1006.
9. Anuradha U, Mehra NK, Khatri DK. Understanding molecular mechanisms and miRNA-based targets in diabetes foot ulcers. Mol Biol Rep. 2024;51(1):82. doi: 10.1007/s11033-023-09074-0, PMID 38183502.
10. Kumari P, Singh V, Kant V, Ahuja M. Current status of 1,4-naphthoquinones and their derivatives for wound healing. European Journal of Medicinal Chemistry Reports. 2024;12:100194. doi: 10.1016/j.ejmcr.2024.100194.
11. Bhattacharya S, Paul B, Biswas GR. Development and evaluation of hydrogel of an anti-fungal drug. Int J Pharm Pharm Sci. 2023;15(10):29-33. doi: 10.22159/ijpps.2023v15i10.48728.
12. Fan R, Cheng Y, Wang R, Zhang T, Zhang H, LI J. Thermosensitive hydrogels and advances in their application in disease therapy. Polymers. 2022;14(12):2379. doi: 10.3390/polym14122379, PMID 35745954.
13. Nair SC, MK, Ramesh K. Antiepileptic rectal hydrogel loaded with carbamazepine rice bran wax microspheres. Asian J Pharm Clin Res. 2017;10(3):264-70. doi: 10.22159/ajpcr.2017.v10i3.16144.
14. Chatterjee S, Hui PC. Review of applications and future prospects of stimuli-responsive hydrogel based on thermo responsive biopolymers in drug delivery systems. Polymers. 2021;13(13):2086. doi: 10.3390/polym13132086, PMID 34202828.
15. Kumar M, Saini M, Parihar L. Preformulation studies of pantoprazole: fundamental part of formulation design. Saudi J Med Pharm Sci. 2022;8(8):370-80. doi: 10.36348/sjmps.2022.v08i08.001.
16. Amin P, Patel M. Preformulation studies of varenicline for formulation and development of a novel orally disintegrating film. J Pharm Res Int. 2023;35(17):31-40. doi: 10.9734/jpri/2023/v35i177388.
17. Khan B, Arbab A, Khan S, Fatima H, Bibi I, Chowdhry NP. Recent progress in thermosensitive hydrogels and their applications in drug delivery area. Med Comm Biomaterials and Applications. 2023;2(3):e55. doi: 10.1002/mba2.55.
18. Supachawaroj N. Polymeric hydrogel containing lidocaine loaded polyelectrolyte complex for dry socket wound dressing. Rangsit University; 2022.
19. QI XJ, XU D, Tian ML, Zhou JF, Wang QS, Cui YL. Thermosensitive hydrogel designed for improving the antidepressant activities of genipin via intranasal delivery. Mater Des. 2021;206:109816. doi: 10.1016/j.matdes.2021.109816.
20. Sampaio TP, Oshiro Junior JA, DA Fonseca NF, DE Medeiros AC. Biological evaluation and compatibility study of oral mucoadhesive hydrogel formulations using schinopsis brasiliensis engler extract and excipients. J Therm Anal Calorim. 2023;148(1):141-58. doi: 10.1007/s10973-022-11504-3.
21. HU J, Liu X, Gao Q, Ouyang C, Zheng K, Shan X. Thermosensitive PNIPAM-based hydrogel crosslinked by composite nanoparticles as rapid wound healing dressings. Biomacromolecules. 2023;24(3):1345-54. doi: 10.1021/acs.biomac.2c01380, PMID 36857757.
22. Chatzitaki AT, Mystiridou E, Bouropoulos N, Ritzoulis C, Karavasili C, Fatouros DG. Semi solid extrusion 3D printing of starch based soft dosage forms for the treatment of paediatric latent tuberculosis infection. J Pharm Pharmacol. 2022;74(10):1498-506. doi: 10.1093/jpp/rgab121, PMID 34468746.
23. Chen IC, SU CY, Chen PY, Hoang TC, Tsou YS, Fang HW. Investigation and characterization of factors affecting rheological properties of poloxamer based thermo sensitive hydrogel. Polymers. 2022;14(24):5353. doi: 10.3390/polym14245353, PMID 36559720.
24. Pham DT, Phewchan P, Navesit K, Chokamonsirikun A, Khemwong T, Tiyaboonchai W. Development of metronidazole loaded in situ thermosensitive hydrogel for periodontitis treatment. Turk J Pharm Sci. 2021;18(4):510-6. doi: 10.4274/tjps.galenos.2020.09623, PMID 34496558.
25. Derkar S, Ingole A, Baheti JR. Formulation and evaluation of herbal antibacterial and antimicrobial gel. World J Pharm Res. 2022;11(3):1656-69.

26. Bercea M, Constantin M, Plugariu IA, Oana Daraba M, Luminita Ichim D. Thermosensitive gels of pullulan and poloxamer 407 as potential injectable biomaterials. J Mol Liq. 2022 Sep 15;362:119717. doi: 10.1016/j.molliq.2022.119717.
27. Shiva K, Mandal S, Kumar S. Formulation and evaluation of topical antifungal gel of fluconazole using aloe vera gel. Int J Sci Res Dev. 2021;6(1):187-93.
28. Gambhire MS, Gambhire VM, Bachhav JR. Formulation development and optimization of mucoadhesive in situ gelling system for nasal administration of piracetam. J Maharaja Sayajirao University Baroda. 2021;55(2):21-31.
29. Parmar PK, Wadhawan J, Bansal AK. Pharmaceutical nanocrystals: a promising approach for improved topical drug delivery. Drug Discov Today. 2021;26(10):2329-49. doi: 10.1016/j.drudis.2021.07.010, PMID 34265460.
30. Syed MA, Aziz G, Jehangir MB, Tabish TA, Zahoor AF, Khalid SH. Evaluating novel agarose based buccal gels scaffold: mucoadhesive and pharmacokinetic profiling in healthy volunteers. Pharmaceutics. 2022;14(8):1592. doi: 10.3390/pharmaceutics14081592, PMID 36015217.
31. Gonzalez Gonzalez O, Ramirez IO, Ramirez BI, O'Connell P, Ballesteros MP, Torrado JJ. Drug stability: ICH versus accelerated predictive stability studies. Pharmaceutics. 2022;14(11):2324. doi: 10.3390/pharmaceutics14112324, PMID 36365143.
32. Chavez Esquivel G, Cervantes Cuevas H, Ybieta Olvera LF, Castaneda Briones MT, Acosta D, Cabello J. Antimicrobial activity of graphite oxide doped with silver against bacillus subtilis candida albicans escherichia coli and staphylococcus aureus by agar well diffusion test: synthesis and characterization. Mater Sci Eng C Mater Biol Appl. 2021;123:111934. doi: 10.1016/j.msec.2021.111934, PMID 33812573.
33. Shelke M, Godge R, Sahane T, Pawar O, Kasar S. Stability indicating Rp-HPLC method for estimation of cariprazine hydrochloride in human plasma. J Appl Pharm Res. 2024;12(2):27-34. doi: 10.18231/j.joapr.2024.12.2.27.34.
34. Nunes D, Andrade S, Ramalho MJ, Loureiro JA, Pereira MC. Polymeric nanoparticles loaded hydrogels for biomedical applications: a systematic review on *in vivo* findings. Polymers. 2022;14(5):1010. doi: 10.3390/polym14051010, PMID 35267833.
35. Galocha Leon C, Antich C, Voltes Martinez A, Marchal JA, Mallandrich M, Halbaut L. Development and characterization of a poloxamer hydrogel composed of human mesenchymal stromal cells (*hMSCs*) for reepithelization of skin injuries. Int J Pharm. 2023;647:123535. doi: 10.1016/j.ijpharm.2023.123535, PMID 37865132.
36. Choi S, Jeon J, Bae Y, Hwang Y, Cho SW. Mucoadhesive phenolic pectin hydrogels for saliva substitute and oral patch. Adv Funct Materials. 2023;33(44):2303043. doi: 10.1002/adfm.202303043.
37. Almawash S, Osman SK, Mustafa G, El Hamd MA. Current and future prospective of injectable hydrogels design challenges and limitations. Pharmaceuticals (Basel). 2022;15(3):371. doi: 10.3390/ph15030371, PMID 35337169.
38. Allolinggi GS, Setyani W. Factorial design optimization of antioxidant cream from kepok banana peel extract: formulation characterization and stability evaluation. Nat Sci Eng Technol J. 2025;5(1):445-57.
39. Caputo F, Mehn D, Clogston JD, Rosslein M, Prina Mello A, Borgos SE. Asymmetric flow field flow fractionation for measuring particle size drug loading and (in)stability of nanopharmaceuticals the joint view of European Union Nanomedicine Characterization Laboratory and National Cancer Institute- Nanotechnology Characterization Laboratory. J Chromatogr A. 2021;1635:461767. doi: 10.1016/j.chroma.2020.461767, PMID 33310281.
40. Cassano R, Di Gioia ML, Trombino S. Gel-based materials for ophthalmic drug delivery. Gels. 2021;7(3):130. doi: 10.3390/gels7030130, PMID 34563016.
41. Elmanawy MA, Boraie N, Bakr BA, Makled S. Augmented ocular uptake and anti-inflammatory efficacy of decorated genistein loaded NLCs incorporated in in situ gel. Int J Pharm. 2024;662:124508. doi: 10.1016/j.ijpharm.2024.124508, PMID 39053680.
42. Bayer IS. Recent advances in mucoadhesive interface materials mucoadhesion characterization and technologies. Adv Materials Inter. 2022;9(18):2200211. doi: 10.1002/admi.202200211.
43. Song Y, Abdella S, Afinjuomo F, Weir EJ, Tan JQ, Hill P. Physicochemical properties of otic products for canine otitis externa: comparative analysis of marketed products. BMC Vet Res. 2023;19(1):39. doi: 10.1186/s12917-023-03596-2, PMID 36759841.
44. Lateef SN, Kendre PS. Oral sustained delivery of theophylline floating matrix tablets formulation and *in vitro* evaluation. Int J Pharm Tech Res. 2010;2(1):130-9.
45. Mathure D, Sutar AD, Ranpise H, Pawar A, Awasthi R. Preparation and optimization of liposome containing thermosensitive in situ nasal hydrogel system for brain delivery of sumatriptan succinate. Assay Drug Dev Technol. 2023;21(1):3-16. doi: 10.1089/adt.2022.088, PMID 36576871.
46. Bhuiyan MH, Clarkson AN, Ali MA. Optimization of thermoresponsive chitosan/β-glycerophosphate hydrogels for injectable neural tissue engineering application. Colloids Surf B Biointerfaces. 2023;224:113193. doi: 10.1016/j.colsurfb.2023.113193, PMID 36773410.
47. Ibrahiem B, Shamma R, Salama A, Refai H. Magnetic targeting of lornoxicam/SPION bilosomes loaded in a thermosensitive in situ hydrogel system for the management of osteoarthritis: optimization, *in vitro*, ex vivo, and *in vivo* studies in rat model via modulation of RANKL/OPG. Drug Deliv Transl Res. 2024;14(7):1982-2002. doi: 10.1007/s13346-023-01503-8, PMID 38158473.
48. Gholami M, Tajabadi M, Khavandi A, Azarpira N. Synthesis optimization and cell response investigations of natural based thermoresponsive injectable hydrogel: an attitude for 3D hepatocyte encapsulation and cell therapy. Front Bioeng Biotechnol. 2022;10:1075166. doi: 10.3389/fbioe.2022.1075166, PMID 36686232.
49. Noreen S, Pervaiz F, Ashames A, Buabeid M, Fahelelbom K, Shoukat H. Optimization of novel naproxen loaded chitosan/carrageenan nanocarrier based gel for topical delivery: ex vivo histopathological and *in vivo* evaluation. Pharmaceuticals (Basel). 2021;14(6):557. doi: 10.3390/ph14060557, PMID 34207951.
50. Panigrahi R, Patro G, Gupta AK, Choudhury A. Development and characterization of tolfenamic acid loaded solid lipid nanoparticles in a topical gel for effective management of inflammatory conditions. Cuest Fisioter. 2025;54(2):2052-67.
51. DE Souza Von Zuben E, Eloy JO, Araujo VH, Gremiao MP, Chorilli M. Insulin-loaded liposomes functionalized with cell penetrating peptides: influence on drug release and permeation through porcine nasal mucosa. Colloids and Surfaces A: Physicochemical and Engineering Aspects. 2021;622. doi: 10.1016/j.colsurfa.2021.126624.
52. Haggag YA, Abdel Wahab M, Eltokhy SS, Elnawasany S, Mabrouk MM, Kenawy ER. Co-delivery of novel valsartan and hydrochlorothiazide pH-responsive electrospun polymeric nanofibers for improved oral delivery. J Drug Deliv Sci Technol. 2024;101:106241. doi: 10.1016/j.jddst.2024.106241.
53. Crommelin DJ, Anchordoquy TJ, Volkin DB, Jiskoot W, Mastrobattista E. Addressing the cold reality of mRNA vaccine stability. J Pharm Sci. 2021;110(3):997-1001. doi: 10.1016/j.xphs.2020.12.006, PMID 33321139.
54. Luiten J, Kopanas G, Leibe B, Ramanan D. Dynamic 3D gaussians: tracking by persistent dynamic view synthesis. International Conference on 3D Vision; 2024. doi: 10.1109/3DV62453.2024.00044.
55. Kuzman D, Bunc M, Ravnik M, Reiter F, Zagar L, Boncina M. Long term stability predictions of therapeutic monoclonal antibodies in solution using arrhenius-based kinetics. Sci Rep. 2021;11(1):20534. doi: 10.1038/s41598-021-99875-9, PMID 34654882.
56. Galgano M, Capozza P, Pellegrini F, Cordisco M, Sposato A, Sblano S. Antimicrobial activity of essential oils evaluated *in vitro* against escherichia coli and staphylococcus aureus.

Antibiotics (Basel). 2022;11(7):979. doi: 10.3390/antibiotics11070979, PMID 35884233.

57. Esteban P, Redrado S, Comas L, Domingo MP, Millan Lou MI, Seral C. *In vitro* and *in vivo* antibacterial activity of gliotoxin alone and in combination with antibiotics against staphylococcus aureus. Toxins. 2021;13(2):85. doi: 10.3390/toxins13020085, PMID 33498622.
58. Xia S, Ma L, Wang G, Yang J, Zhang M, Wang X. *In vitro* antimicrobial activity and the mechanism of berberine against methicillin resistant staphylococcus aureus isolated from bloodstream infection patients. Infect Drug Resist. 2022;15:1933-44. doi: 10.2147/IDR.S357077, PMID 35469308.
59. Kebede B, Shibeshi W. *In vitro* antibacterial and antifungal activities of extracts and fractions of leaves of *Ricinus communis* linn against selected pathogens. Vet Med Sci. 2022;8(4):1802-15. doi: 10.1002/vms3.772, PMID 35182460.
60. Barreiros Y, Meneses AC, Alves JL, Mumbach GD, Ferreira FA, Machado RA. Xanthan gum based film forming suspension containing essential oils: production and *in vitro* antimicrobial activity evaluation against mastitis causing microorganisms. LWT. 2022;153:112470. doi: 10.1016/j.lwt.2021.112470.
61. Selvanathan V, Aminuzzaman M, Tan LX, Win YF, Guan Cheah ES, Heng MH. Synthesis characterization and preliminary *in vitro* antibacterial evaluation of ZnO nanoparticles derived from soursop (*Annona muricata L.*) leaf extract as a green reducing agent. J Mater Res Technol. 2022;20:2931-41. doi: 10.1016/j.jmrt.2022.08.028.
62. Padma Prashanthini V, Sivaraman S, Kathirvelu P, Shanmugasundaram J, Subramanian V, Ramesh SS. Transferosomal gel for transdermal delivery of insulin: formulation development and ex vivo permeation study. Intelligent Pharmacy. 2023;1(4):212-6. doi: 10.1016/j.ipha.2023.07.001.
63. Gonzalez Gonzalez O, Ramirez IO, Ramirez BI, O Connell P, Ballesteros MP, Torrado JJ. Drug stability: ICH versus accelerated predictive stability studies. Pharmaceutics. 2022;14(11):2324. doi: 10.3390/pharmaceutics14112324, PMID 36365143.
64. Caputo F, Mehn D, Clogston JD, Rosslein M, Prina Mello A, Borgos SE. Asymmetric flow field flow fractionation for measuring particle size drug loading and (in)stability of nanopharmaceuticals the joint view of European Union Nanomedicine Characterization Laboratory and National Cancer Institute Nanotechnology Characterization Laboratory. J Chromatogr A. 2021;1635:461767. doi: 10.1016/j.chroma.2020.461767, PMID 33310281.